PHYSICAL REVIEW APPLIED **14,** 034008 (2020)

Large Piezoelectriclike Response from Inhomogeneously Deformed Silicon Crystals

Dongxia Tian, Yu Hou, Qi Pan, and Baojin Chu[*]
CAS Key Laboratory of Materials for Energy Conversion and Department of Materials Science and Engineering, University of Science and Technology of China, Heifei 230026, China

(Received 3 March 2020; revised 17 June 2020; accepted 17 August 2020; published 2 September 2020)

Silicon (Si) crystals are important materials for the modern microelectronics industry. While Si crystals are not piezoelectric materials due to their centrosymmetric structure, it is found in this work that Si crystals exhibit a large piezoelectric-like response under bending deformation. We show that this response is not intrinsic, but rather originates from the surfaces of crystals that are slightly oxidized upon their exposure to air. The weak piezoelectric response of the surface is amplified by high conductivity of the bulk and bending deformation of Si plates. In addition, the piezoelectric-like response is strongly dependent on the conduction type and the resistivity of the crystals and on the metal electrode used for piezoelectric measurements. A multilayer model is proposed to explain the piezoelectric-like response of the Si crystals. This finding may be exploited to design piezoelectric devices using Si only, without the integration of additional piezoelectric materials, and is important for understanding the Si crystal surfaces.

DOI: 10.1103/PhysRevApplied.14.034008

I. INTRODUCTION

Piezoelectric materials generate an electrical response due to an applied mechanical stress and vice versa [1–5]. These materials are used in a wide range of applications, such as sensors, actuators, transducers, and energy-harvesting devices. In addition to bulk piezoelectric materials that have been widely used in many applications, microelectromechanical systems have become mainstream devices in applications due to their small size, high integration density, and multifunctionality [6–10]. For compatibility with current semiconductor device technology, piezoelectric thin films are often fabricated on semiconductor substrates, which, in most cases, are Si crystals. The integration of piezoelectric materials, many of which are oxides, with Si crystals requires advanced fabrication techniques and complex procedures to achieve high-performance devices and has been a subject of intense research [9,10].

For the piezoelectric effect to exist, the crystal structure of a material should not have a center of symmetry [1]. While some III-V and II-VI semiconductors are piezoelectrics, Si crystals that form the basis of the current microelectronics industry should not exhibit the piezoelectric effect because of their face-centered-cubic crystal structure [11–13]. Similar to piezoelectric materials, Si crystals can be used to detect mechanical stress, but this is realized by exploiting the piezoresistance effect, which is the change of electrical resistance under a mechanical load [14–17]. Unlike piezoelectric devices, an external power source is required for measurements of the resistivity change in piezoresistive devices. Thus, the integration of a piezoelectric thin film on Si to obtain a piezoelectric device can simplify the design of a stress sensor [9,10].

Here, we demonstrate that, although Si crystals are not piezoelectric materials, a Si crystal plate can generate a strong piezoelectric-like response under bending deformation. We show that the piezoelectric-like response originates mainly from the surface of the Si crystals. This discovery is important for understanding the nature of the surface of Si crystals. The observed piezoelectric-like response can also be explored for potential applications in piezoelectric devices.

II. EXPERIMENTAL METHODS

The n-type and p-type Si wafers [(100) oriented and (111) oriented] with different resistivity values are purchased from Suzhou Crystalline Silicon Electronic Technology (Suzhou, China). The n-type polycrystalline Si is obtained from Dalian University of Technology. The resistivity of the Si wafers is measured using a four-probe measurement system (RTS-8, four-probe technology, Guangzhou, China). For (100)-oriented Si, the resistivity values of the n-type wafers are 3, 4, 3700, and 15 500 Ω cm, and those of the p-type wafers are 8 and 5700 Ω cm. The resistivity of (111)-oriented n-type Si is 9 Ω cm and that of n-type polycrystalline Si is 4 Ω cm. The Si wafers are cut into rectangular plates with a length,

---

[*] chubj@ustc.edu.cn

width, and thickness of 30, 4.5, and 0.5 mm, respectively. Gold electrodes are sputtered onto the top and bottom surfaces of the plates using a sputter coater (EMS150T, Electron Microscopy Sciences, Hatfield, PA, USA) prior to the piezoelectric measurements. Other types of electrodes, namely, Pt, Ag, and Al, are deposited using an electron-beam evaporator (K. J. Lesker, LAB 18, USA). To measure the electromechanical response, the silicon plates are supported at the two ends, and a dynamic force (110 Hz) from a quasi-static d_{33} meter (ZJ-6A, Institute of Acoustics, CAS, Beijing, China) is applied at the center of the samples [the three-point bending (TPB) approach], as shown schematically in Fig. 1(a). Under bending deformation, a piezoelectric-like response is generated by the Si plates. The response can be directly read from the d_{33} meter. In the measurement of the piezoelectric response by the d_{33} meter, the piezoelectric charge is determined by a capacitor in parallel to the piezoelectric materials. The capacitance of the piezoelectric materials should be much smaller than that of the capacitor to enable accurate charge measurements. Since the capacitance values of some Si samples used in our study are comparable to that of the capacitor for charge measurements, the measured d_{33} is corrected after measurements (see the Supplemental Material for a detailed explanation [18]). Prior to electrode deposition and piezoelectric measurements, the as-received Si wafers are etched with a solution of NH_4F-HF solution [a mixture of NH_4F solution (40%) and HF solution (49%), at a mixing ratio of 6:1] for about 2 min. Some of the Si crystals are abraded with polishing papers (particle size 20–28 μm) at room temperature for comparison. For NH_4F-HF-etched Si plates, the gold electrode is sputtered on the surface of the plate after exposure to air for 2 h. The piezoelectric-like response (effective d_b) is measured after the electromechanical response is stabilized after 24 h. To study the effect of abrasion on the piezoelectric-like response, the

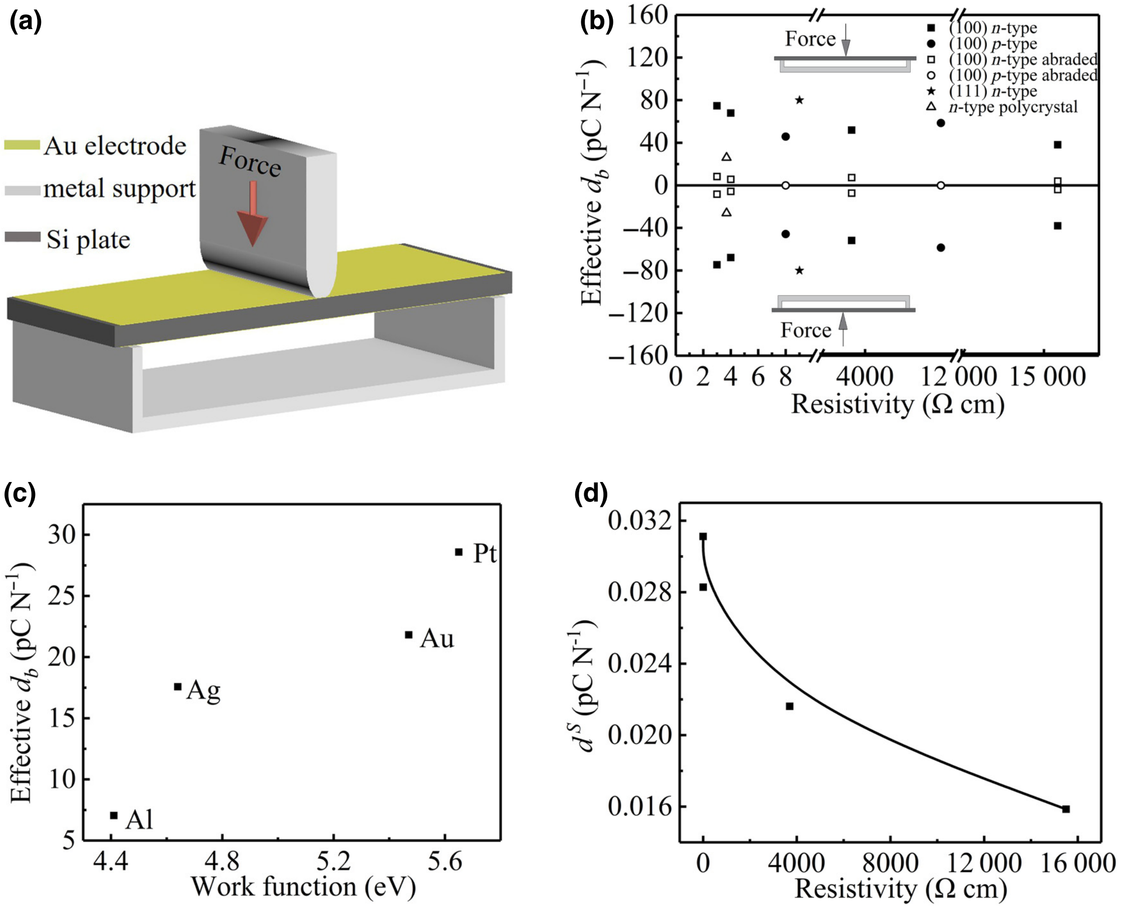

FIG. 1. Piezoelectric-like response of *n*-type and *p*-type Si plates under TPB load. (a) Schematic for the measurement of the piezoelectric-like response of the Si plate using the TPB approach. (b) Piezoelectric-like response of Si plates with different resistivity values before and after abrading. Electrode used for the measurement is sputtered Au. Effective d_b is measured under opposite bending directions by flipping over the Si plate and the test fixture, as schematically shown in the inset. (c) Piezoelectric-like response of *n*-type Si plates [(100) oriented and resistivity 3 Ω cm] coated with different metal electrodes prepared by electron-beam evaporation. (d) Calculated piezoelectric response of the surface of *n*-type Si plates with different resistivity values [(100) oriented].

abraded Si plates are sputtered with a gold electrode immediately after abrasion and the effective d_b is then measured. To observe the effect of the SiO_2 layer on the electromechanical response, SiO_2 films with different thicknesses (5, 10, 20, and 60 nm) are deposited using a plasma-enhanced chemical vapor deposition (PECVD) system (Plasma Pro System 100, Oxford, UK). The surface chemistry of the Si crystals is examined by x-ray photoelectron spectroscopy (XPS, Escalab 250, Thermo Fisher Scientific, UK). The work function of the metal electrode was measured by ultraviolet photoelectron spectroscopy (UPS, Escalab 250, Thermo Fisher Scientific, UK). X-ray diffraction (XRD) is measured by a Rigaku Smartlab diffractometer (Rigaku, Tokyo, Japan).

III. RESULTS AND DISCUSSION

The piezoelectric coefficient d_{33} (the ratio of the generated electric charge to the applied force) of piezoelectric materials is usually evaluated using a commercial d_{33} meter. In these measurements, a dynamic force is applied to the materials by two-point probes, and the piezoelectric coefficient d_{33} can be directly read from the equipment [19]. When a Si plate is placed between the point probes of a d_{33} meter, a d_{33} value in the range of 5–8 $\mathrm{pC\,N^{-1}}$ is obtained. After the plate is turned upside down, a d_{33} value of the same magnitude and sign is obtained. Because the sign of d_{33} does not change with the orientation of the Si plate, the measured d_{33} is not due to the piezoelectric effect, but rather is due to the high conductivity of the Si crystals (see the Supplemental Material for a detailed explanation [18]). However, when a TPB load is applied to the plate using the sample configuration shown in Fig. 1(a), a large d_{33} value is measured. After the bending direction is changed by turning the Si plate and the test fixture upside down, the d_{33} value changes sign and shows a smaller absolute value (see Table S1 within the Supplemental Material [18]). The sign change indicates that the measured d_{33} is not due to the conductivity, but rather arises from a true piezoelectric response. The difference in the absolute values of d_{33} under opposite bending directions can be attributed to the spurious signal due to the conductivity of the sample. The conductivity contribution to the value of d_{33} is determined by placing the plate between the two-point probes of the d_{33} meter, without applying the TPB load, and subtracting this value from that of d_{33} measured under the TPB load. After subtraction, the absolute d_{33} values measured from opposite bending directions are almost identical (Table S1 within the Supplemental Material [18]). Those values represent the true piezoelectric-like response from the bent Si plates. The effective d_b values of the n-type Si plates [(100) oriented] under the TPB load are summarized in Fig. 1(b), which are in the range of 35–75 $\mathrm{pC\,N^{-1}}$, and decrease with increasing resistivity of the Si crystals. In addition to the n-type Si crystals, the effective d_b of the p-type Si crystals [(100) oriented] is measured. As shown in Fig. 1(b), the effective d_b of the p-type Si crystals exhibits a different variation trend with resistivity from that of the n-type Si crystals. In contrast to the n-type Si crystals, the effective d_b of the p-type Si crystals increases with resistivity. Also, the effective d_b is smaller than that of the n-type Si crystals at low resistivity.

Because Si crystals are not piezoelectric materials, it is unusual to observe a large piezoelectric-like response in the crystals under a TPB load. The origin of the piezoelectric-like response is further explored. The results shown in Fig. 1(b) indicate that, overall, the effective d_b of the n-type Si crystals is larger than that of the p-type Si crystals. Because the electron affinity of Si is about 4.1 eV and the band gap is about 1.1 eV, n-type Si forms a Schottky contact with the Au (work function $W \sim 5.1$ eV) electrode [13]. On the other hand, for p-type Si, an Ohmic contact should be formed between Si and the Au electrode. The difference in the effective d_b between the n-type and p-type Si crystals implies that the formation of a Schottky contact is important for achieving a higher piezoelectric-like response. This conclusion is further supported by the measurement of a piezoelectric-like response in the n-type Si plates [(100) oriented and resistivity 3 Ω cm] coated with different metal electrodes. As shown in Fig. 1(c), the effective d_b of the n-type Si plates is about 29 $\mathrm{pC\,N^{-1}}$ when Pt ($W \sim 5.6$ eV) is deposited as the electrode. The effective d_b then decreases with the decreasing work function of the electrode and is reduced to about 7 $\mathrm{pC\,N^{-1}}$ when Al ($W \sim 4.45$ eV) is used as the electrode. By reducing the electrode work function, the contact between Si and the metal electrode changes from a Schottky contact to an Ohmic contact [13]. Accordingly, the effective d_b will approach a value close to zero when a metal with a low work function is used as the electrode.

We also discover that the surface of Si plays an important role in the observed piezoelectric-like response. The Au electrodes used in this work are mostly fabricated by the sputtering method, while the Pt, Ag, and Al electrodes are deposited by the electron-beam evaporation method. When the Au electrode is deposited on the Si plates by the electron-beam evaporation method, the effective d_b is significantly reduced. For example, the effective d_b of the n-type Si plate with a resistivity of 3 Ω cm is 22 $\mathrm{pC\,N^{-1}}$, as shown in Fig. 1(c), which is smaller than that measured for the same plate with the sputtered Au electrode [effective $d_b \sim 75$ $\mathrm{pC\,N^{-1}}$, Fig. 1(b)]. Because different electrode deposition processes affect only the surface of the Si crystals, this result reveals that the surface of Si crystals has a significant effect on the measured piezoelectric-like response. Therefore, the role of the surface in the observed piezoelectric-like response is investigated. For the above-described piezoelectric measurements, the Si plates are subjected to NH_4F-HF etching and exposed to the atmosphere for approximately 2 h prior to electrode deposition. It is found that, when the surface of the Si plates [(100) oriented] is abraded with sandpaper, and the Au electrode is deposited rapidly to minimize the exposure time in air, the piezoelectric-like response of the bent Si plates is significantly reduced, as shown in Fig. 1(b). For example, the effective d_b of the abraded n-type Si plate with a resistivity of 3 Ω cm is only 8 pC N^{-1}, whereas that of the nonabraded Si plate with the same resistivity is about 75 pC N^{-1} [Fig. 1(b)]. However, for p-type Si plates, the effective d_b is reduced to about 0 pC N^{-1} after abrasion. The significant effect of abrasion on the piezoelectric-like response of the bent Si plates suggests that the response is not an intrinsic property of Si crystals, but primarily originates from the Si surface.

We start by assuming that the two surface layers possess a piezoelectric effect to generate the observed piezoelectric-like response in the sample and propose a multilayer model to explain the mechanism for the piezoelectric-like response of the bent Si plate, as schematically shown in Fig. 2. A possible origin of the piezoelectricity at the surfaces is discussed later. Because the two opposite surfaces are symmetric, the signs of the piezoelectric response from the two surfaces should be opposite, and the magnitude of the response should be equal if a uniform load is applied. The responses from the two surfaces should cancel each other out under uniform deformation. Because one surface is in tension and the other surface is in compression under a nonuniform bending deformation, the responses of the two surfaces lead to a nonzero total piezoelectric response. For n-type Si, after the formation of a Schottky contact with the Au electrode, two depletion layers that are more insulating than the bulk are present adjacent to the piezoelectric surface layers. These depletion layers are absent in p-type Si. Because the surface layer can be very thin (as discussed below), the tunneling mechanism becomes an important conduction mechanism and the layer might not be very insulating [20,21]. In n-type Si, the depletion layers separate the piezoelectric surfaces from the highly conductive bulk, protecting the piezoelectric charge of the surfaces from being screened by the free charge from the bulk, which can increase the piezoelectric response of the surfaces. This explains why the n-type Si crystals generally show a larger piezoelectric-like response than that of p-type Si crystals. A comparison of the piezoelectric-like response between the abraded n-type crystals and p-type Si crystals suggests that the two depletion layers may have a weak piezoelectric response, which most likely arises from the space-charge layer in the depletion layer [22]. However, it is also possible that abrasion cannot eliminate the piezoelectric surface completely. In p-type Si crystals, because the piezoelectric surface after abrasion is so thin that the piezoelectric charge from the surface can be easily screened by the free charge, no piezoelectric response can be measured [Fig. 1(b)]. On the other hand, in n-type Si crystals, the piezoelectric response is protected by the insulating depletion layers, and hence, a weak piezoelectric response is still measured. In this case, the depletion layer may not possess a piezoelectric effect and the piezoelectric-like response in abraded n-type Si plates is also due to the surface. The remaining portion of the crystal is the nonpiezoelectric and conductive bulk. Because of high conductivity, free charge in the bulk can compensate for the piezoelectric charge generated by the surface layer, which is equivalent to the generation of a polarization response similar to that from the piezoelectric surface and improves the overall polarization response. This phenomenon is similar to the barrier-layer effect in dielectrics [23,24]. The piezoelectric response from the surface is further enhanced because of the bending deformation of the Si plates (see the Supplemental Material for a detailed explanation [18]), leading to the measured large piezoelectric-like response.

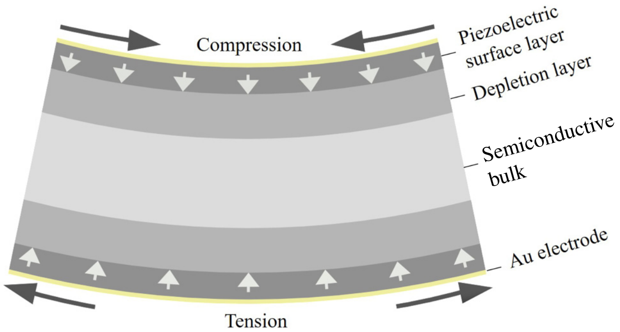

FIG. 2. Schematic of the multilayer model proposed to explain the observed piezoelectric-like response of the Si plates under bending deformation. Arrows in the surface layers indicate the polarity of the surface piezoelectric response.

Using the proposed multilayer structure shown in Fig. 2, the magnitude of the piezoelectric response of the surface d^S can be estimated using the measured effective d_b of the bent Si plates (see the Supplemental Material [18]) according to

$$d^S = \frac{2d_b h^2}{3l^2}, \tag{1}$$

where h (0.0005 m) and l (0.02 m) are the thickness and length of the Si plates, respectively. Using the data in Fig. 1(b) and Eq. (1), the d^S values are estimated for the n-type Si crystals [(100) oriented] with different resistivity values and the results are shown in Fig. 1(d). It is found that d^S of the n-type Si crystals is in the range of 0.016–0.032 pC N^{-1}, which is much lower than the response measured in many well-studied piezoelectric materials (for example, $BaTiO_3$ ceramics, $d_{33} \sim 190$ pC N^{-1} [25]). It is also observed from Fig. 1(d) that d^S decreases with increasing resistivity of the Si crystals. Based on the proposed multilayer structure shown in Fig. 2, this can be understood as follows. The combination of the depletion layer and the surface layer can be treated as a composite. Because the depletion layer is either nonpiezoelectric or has only a weak piezoelectric response, this layer reduces the effective piezoelectric response from the surface. The thickness of the depletion layer x_d can be estimated by [26]

$$x_d = \sqrt{\frac{2\varepsilon_s\varepsilon_0}{qN_D}\left(V_D - \frac{k_0T}{q}\right)}, \tag{2}$$

where V_D is the built-in potential in the depletion layer; k_0 is the Boltzmann constant; T is the temperature; q is the electron charge; ε_s and ε_0 are the dielectric constant of Si and the vacuum permittivity, respectively; and N_D is the donor concentration of the n-type Si crystals. For the n-type Si crystals used in this study, N_D is in the range of 1×10^{21} to 1×10^{17} m^{-3} [27], and ε_s ($\sim$11) is assumed not to be dependent on the dopant concentration [28]. It is clear that x_d increases with increasing resistivity, resulting in a reduction of d^S with increasing resistivity.

Our results also reveal that the piezoelectric surface cannot be eliminated, even when an additional layer of SiO_2 films is intentionally deposited on the surface of the n-type Si plates. Because the deposited SiO_2 films are amorphous, they should not exhibit a piezoelectric response. The addition of the SiO_2 layer further reduces the effective piezoelectric response d^S_{eff}, similar to the effect of the depletion layer. The d^S_{eff} value after deposition of the SiO_2 films is related to the thickness, x_f, of the SiO_2 films, according to (see the Supplemental Material [18])

$$d^S_{\mathrm{eff}} = d^S \frac{t_S}{x_f}, \tag{3}$$

where t_S is the thickness of the piezoelectric surface layer. Figure 3 shows the dependence of the piezoelectric-like response of the n-type Si plates [(100) oriented and resistivity 3 Ω cm] under a TPB load on the thicknesses of the deposited SiO_2 films. The effective d_b decreases with an increase of the thickness of the SiO_2 films, and the two parameters roughly follow the inversely proportional relationship expected from Eq. (3).

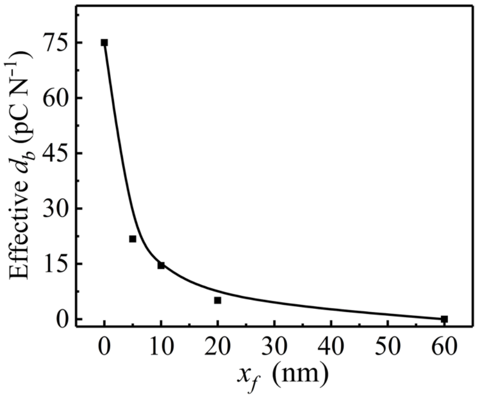

FIG. 3. Dependence of the piezoelectric-like response of the bent Si plates [(100) oriented and resistivity 3 Ω cm] on the thicknesses of the deposited SiO_2 films.

The origin of the piezoelectric effect observed for the surface of the Si crystals is investigated. Because the piezoelectric-like response of bent Si plates is strongly dependent on abrasion of the surface, we speculate that the piezoelectric surface may be produced by the interaction between the Si crystals and surrounding environment. An analysis of the surface chemistry by XPS indicates that there exists an oxidation layer on the Si surface, as shown in Fig. 4(a), where the peak at about 102.75 eV is assigned to oxidized Si [29,30]. Previous studies have shown that, upon exposure to air, Si crystals are easily oxidized, even at room temperature [31]. While it is generally believed that SiO_2 obtained by the oxidation process is amorphous, it is possible that, because the thin oxidized layer grows on the Si crystals, it may possess a certain ordering in the vicinity of the surface. This leads to a weak piezoelectric effect in the surface because crystalline SiO_2 is a well-known piezoelectric material. If the oxidized surface is sufficiently thick, it can also function as an insulating layer that protects the piezoelectric charge from the surface from being

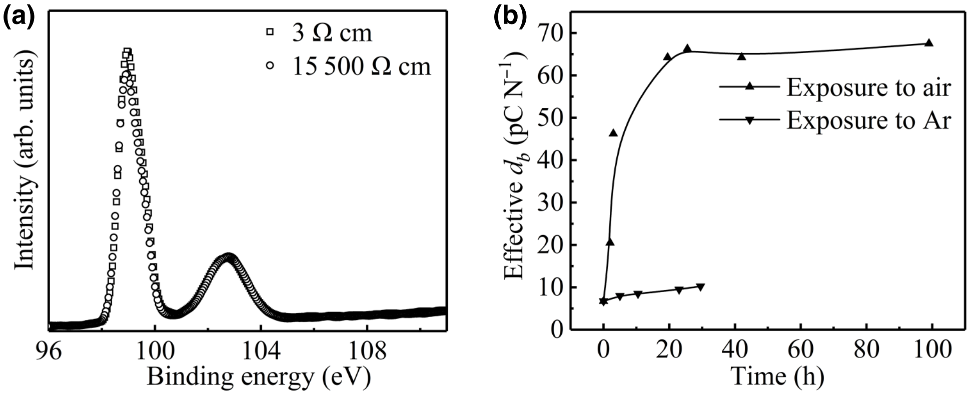

FIG. 4. (a) XPS of the surface of n-type Si [(100) oriented] with resistivities of 3 and 15 500 Ω cm. (b) Time dependence of piezoelectric-like response of the bent n-type Si plates [(100) oriented and resistivity 3700 Ω cm] exposed to air or Ar after etching and sputtering with Au electrode.

screened by the conduction charge. This is the reason why the piezoelectric-like response can also be observed in the nonabraded p-type Si plates in which the depletion layer is absent.

The argument that the piezoelectric response from the Si surface originates from the oxidization of the surface is further supported by the observation that the response is strongly dependent on the exposure time of the Si crystals in air. After the surface of a piece of n-type Si plate [(100) oriented and resistivity 3700 Ω cm] is etched by NH_4F-HF, the plate is exposed to air for 2 h before the gold electrode is sputtered on the surface. After that, the time dependence of the effective d_b is measured. As shown in Fig. 4(b), the effective d_b initially increases with time and reaches a nearly constant value after exposure to air for approximately 24 h. However, if the etched Si plate is protected from exposure to air by sealing the plate in Ar gas after etching, except for the short exposure time in air during the piezoelectric measurement and transfer of the sample, the effective d_b is much reduced, as shown in Fig. 4(b). The result reveals that the piezoelectric response of the surface of the Si crystals is indeed generated during exposure to air. From Fig. 4(b), we notice that the sputtered gold electrode cannot completely protect the Si surface from exposure to air probably because the gold layer prepared by sputtering is thin (estimated to be <100 nm) and not dense.

In addition to (100)-oriented Si, the piezoelectric-like response of the (111)-oriented n-type Si crystal (resistivity 9 Ω cm) and n-type polycrystalline Si (resistivity 4 Ω cm) is also measured, and the results are shown in Fig. 1(b). A d_b of about 80 $\mathrm{pC\,N^{-1}}$ is obtained in (111)-oriented Si crystals. The response is larger than the d_b of (100)-oriented Si with similar resistivity. One possible explanation is that, because the (111) plane is close packed in Si crystals, more Si atoms can be oxidized (more polar Si—O bonds), resulting in a larger piezoelectric response near the surface. For polycrystalline Si, the measured d_b ($\sim$26 $\mathrm{pC\,N^{-1}}$) is much smaller than that of single-crystalline Si with similar resistivity. On the sample surface, similar to single-crystalline Si, each grain still has a polarity, but different grains have different orientations. This may reduce the observed piezoelectric-like response of polycrystalline Si. It should be noted that the grain size of polycrystalline Si is often large (typically >1 mm) and, for the samples used in this study, the grain size is in the millimeter range, which is comparable to the size of the samples used for piezoelectric measurement. Consequently, the grains in polycrystalline Si cannot be thought to be randomly oriented, and the overall piezoelectric response is determined by the dominant equivalent orientation of the samples.

The generation of the electric response under bending deformation in Si crystals is similar to the flexoelectric effect observed in dielectric materials [32–41]. However, the flexoelectric effect should not be an important mechanism for the observed piezoelectric-like response in bent Si plates. This conclusion is supported by the fact that the piezoelectric-like response of bent Si plates is significantly reduced by abrasion. Furthermore, for abraded p-type Si plates, almost no piezoelectric-like response can be measured. If the flexoelectric response is a major mechanism for the measured piezoelectric-like response, the effective d_b measured in abraded p-type Si crystals should not be zero. Although a modeling study indicates that the flexoelectric response from the bulk can be affected by the change of surface polarization by a factor of two [42], the large variation of effective d_b by abrasion (as high as 10 times) cannot be explained by the change of flexoelectric response caused by the change of surface polarization state. The flexoelectric mechanism is also difficult to explain the large variation of the effective d_b by the change of doping, which leads to n-type and p-type Si with different resistivity values, and the change of electrode materials.

To support the conclusion that the flexoelectric effect is not a major mechanism for the piezoelectric-like response in bent Si plate, the magnitude of the response from the flexoelectric effect is estimated. The bulk static flexoelectric coefficient, μ, of Si can be roughly estimated by [32,37,38]

$$\mu = \chi \frac{q}{a}, \tag{4}$$

where χ is the dielectric susceptibility of Si and a is the dimension of the unit cell of Si. The size of the unit cell of Si crystals is 5.43×10^{-10} m, as determined by XRD (see the Supplemental Material [18]). The value of μ of Si is estimated to be about $3 \times 10^{-9}\ \mathrm{C\,m^{-1}}$. The magnitude of the estimated coefficient is consistent with the modeling result for Si crystals, which is typically around or below 1 $\mathrm{nC\,m^{-1}}$ [43]. Under bending, the flexoelectric response can generate a piezoelectric-like response, and the effective d_b from the flexoelectricity can be calculated by [44]

$$d_\mathrm{b} = \frac{3\mu'_{12} l^2}{2\mathrm{c}_{11} h^3}. \tag{5}$$

For (100) Si crystals, $c_{11} = 1.69 \times 10^{11}$ Pa [45]. The effective flexoelectric coefficient μ'_{12} in Eq. (5) includes the contribution from the transverse flexoelectric coefficient μ_{12} and the longitudinal flexoelectric coefficient μ_{11}, but mainly from μ_{12} under bending deformation [44]. If we assume μ'_{12} is equal to μ_{12} and is overestimated to be 5 $\mathrm{nC\,m^{-1}}$, the calculated effective d_b is about 0.15 $\mathrm{pC\,N^{-1}}$ using Eq. (5), which is much lower than the measured effective d_b (typically >10 $\mathrm{pC\ N^{-1}}$ and can be as high as 75 $\mathrm{pC\,N^{-1}}$). Consequently, the contribution of the flexoelectric effect to the reported effective d_b is small. In addition to the bulk static flexoelectric response, the surface piezoelectricity, which is often included in the flexoelectric response, has a similar magnitude to that of the bulk flexoelectric response [33,34]. Therefore, the contribution of surface piezoelectricity to the reported effective d_b is also negligible.

IV. CONCLUSION

We discover that, under bending deformation, a piezoelectric-like electromechanical response can be measured in nonpiezoelectric Si crystals. Experimental results indicate that the piezoelectric-like response is not intrinsic, but originates mainly from the surface of the Si crystals. The piezoelectric effect from the surface may be produced by the oxidation of Si crystals upon their exposure to the atmosphere. In addition to the piezoelectric surface, the depletion layer, after the formation of the Schottky contact between the Si crystals and the metal electrode, is important for achieving a stronger piezoelectric-like response. The depletion layer may protect the charge generated by the piezoelectric surface from being screened by the conduction charge because the surface layer is thin. The conductive Si bulk also plays an important role in the observed piezoelectric-like response, and the weak piezoelectric response from the surface is amplified by the high conductivity of the bulk. Our finding has significant technical and fundamental implications. Most importantly, it is possible that micro- or nanoscale electromechanical devices can be directly designed and fabricated using Si crystals, without the integration of other piezoelectric materials, simplifying the design of these devices. Our study also provides an in-depth understanding of the nature of the surface of Si crystals, which is important for the fabrication of high-performance semiconductor devices.

ACKNOWLEDGMENTS

This research is supported by the National Natural Science Foundation of China (Grants No. 51972297 and No. 51672261) and the National Key Research and Development Program of China (Grant No. 2017YFA0701301). This work is partially carried out at the USTC Center for Micro and Nanoscale Research and Fabrication and Dalian University of Technology.

[1] B. Jaffe, W. R. Cook, and H. Jaffe, *Piezoelectric Ceramics* (Academic, London, 1971).

[2] A. Pramanick, D. Damjanovic, J. C. Nino, and J. L. Jones, Subcoercive cyclic electrical loading of lead zirconate titanate ceramics I: Nonlinearities and losses in the converse piezoelectric effect, J. Am. Ceram. Soc. **92**, 2291 (2009).

[3] S. J. Zhang and F. P. Yu, Piezoelectric materials for high temperature sensors, J. Am. Ceram. Soc. **94**, 3153 (2011).

[4] G. H. Haertling, Ferroelectric ceramics: History and technology, J. Am. Ceram. Soc. **82**, 797 (1999).

[5] J. Rödel, W. Jo, K. T. P. Seifert, E. M. Anton, T. Granzow, and D. Damjanovic, Perspective on the development of lead-free piezoceramics, J. Am. Ceram. Soc. **92**, 1153 (2009).

[6] M. Bao and W. Wang, Future of microelectromechanical systems (MEMS), Sens. Actuators, A **56**, 135 (1996).

[7] J. W. Judy, Microelectromechanical systems (MEMS): Fabrication, design and applications, Smart Mater. Struct. **10**, 1115 (2001).

[8] S. C. Masmanidis, R. B. Karabalin, I. D. Vlaminck, G. Borghs, M. R. Freeman, and M. L. Roukes, Multifunctional nanomechanical systems via tunably coupled piezoelectric actuation, Science **1144793**, 317 (2007).

[9] C. B. Eom and S. Trolier-McKinstry, Thin-film piezoelectric MEMS, MRS Bull. **37**, 1007 (2012).

[10] S. H. Baek, J. Park, D. M. Kim, V. A. Aksyuk, R. R. Das, S. D. Bu, D. A. Felker, J. Lettieri, V. Vaithyanathan, S. S. N. Bharadwaja, and N. Bassiri-Gharb, Giant piezoelectricity on Si for hyperactive MEMS, Science **334**, 958 (2011).

[11] K. W. Chung, Z. Wang, J. C. Costa, F. Williamson, P. P. Ruden, and M. I. Nathan, Barrier height change in GaAs schottky diodes induced by piezoelectric effect, Appl. Phys. Lett. **59**, 1191 (1991).

[12] D. L. Smith and C. Mailhiot, Optical Properties of Strained-Layer Superlattices with Growth Axis Along [111], Phys. Rev. Lett. **58**, 1264 (1987).

[13] K. Huang, *Semiconductor Physics Fundamentals* (Science Press, Beijing, 1979).

[14] C. S. Smith, Piezoresistance effect in germanium and silicon, Phys. Rev. **94**, 42 (1954).

[15] R. R. He and P. D. Yang, Giant piezoresistance effect in silicon nanowires, Nat. Nanotechnol. **1**, 42 (2006).

[16] A. Partridge, J. K. Reynolds, B. W. Chui, E. M. Chow, A. M. Fitzgerald, L. Zhang, N. I. Maluf, and T. W. Kenny, A high-performance planar piezoresistive accelerometer, J. Microelectromech. Syst. **9**, 58 (2000).

[17] D. M. Newns, B. G. Elmegreen, X. H. Liu, and G. J. Martyna, High response piezoelectric and piezoresistive materials for fast, low voltage switching: Simulation and theory of transduction physics at the nanometer-scale, Adv. Mater. **24**, 3672 (2012).

[18] See the Supplemental Material at http://link.aps.org/supplemental/10.1103/PhysRevApplied.14.034008 for additional information about the measurements of piezoelectric response by a d_{33} meter, subtraction of the conduction contribution from measured d_{33}, correction of d_{33} measurement using a d_{33} meter, generation of the piezoelectric-like response from the surface, derivation of the relationship between the piezoelectric-like response of a bent Si plate and piezoelectric response of the surface, and effect of an additional SiO_2 layer on the effective piezoelectric response from the surface and related supplemental data. Refs. [46] and [47] are also included.

[19] C. Pan, *Handbook of a Quasi-Static d_{33} Meter* (IACAS press, Beijing, 2015).

[20] E. H. Rhoderick and R. H. Williams, *Metal Semiconductor Contacts*, 2nd ed. (Clarenden Press, Oxford, 1988).

[21] A. Y. C. Yu, Electron tunneling and contact resistance of metal-silicon contact barriers, Solid-state. Electron. **13**, 239 (1970).

[22] J. H. T. Ransley, A. Aziz, C. Durkan, and A. A. Seshia, Silicon depletion layer actuators, Appl. Phy. Lett. **92**, 184103 (2008).

[23] J. Narvaez, F. Vasquez-Sancho, and G. Catalan, Enhanced flexoelectric-like response in oxide semiconductors, Nature (London) **538**, 219 (2016).

[24] A. J. Moulson and J. M, *Herbert, Electroceramics: Materials, Properties, Applications* (Wiley, New York, 2003).

[25] R. Bechmann, Elastic, piezoelectric, and dielectric constants of polarized barium titanate ceramics and some applications of the piezoelectric equations, J. Acoust. Soc. Am. **28**, 347 (1956).

[26] S M Sze, *Physics of Semiconductor Devices* (Wiley, New York, 1981).

[27] C. Bulucea, Recalculation of irvin's resistivity curves for diffused layers in silicon using updated bulk resistivity data, Solid-state. Electron. **36**, 489 (1993).

[28] S. D. Ristić, Z. D. Prijić, and SŽ Mijalković, Phys. Stat. Sol. (a) **148**, 575 (1995).

[29] Z. H. Lu, J. P. McCaffrey, B. Brar, G. D. Wilk, R. M. Wallace, L. C. Feldman, and S. P. Tay, Sio_2 film thickness metrology by x-ray photoelectron spectroscopy, Appl. Phy. Lett. **71**, 2764 (1997).

[30] K. J. Kim, K. T. Park, and J. W. Lee, Thickness measurement of SiO_2 films thinner than 1 nm by X-ray photoelectron spectroscopy, Thin Solid Films **500**, 356 (2006).

[31] M. Morita, T. Ohmi, E. Hasegawa, M. Kawakami, and M. Ohwada, Growth of native oxide on a silicon surface, J. Appl. Phy. **68**, 1272 (1990).

[32] L. E. Cross, Flexoelectric effects: Charge separation in insulating solids subjected to elastic strain gradients, J. Mater. Sci. **41**, 53 (2006).

[33] P. V. Yudin and A. K. Tagantsev, Fundamentals of flexoelectricity in solids, Nanotechnology **24**, 432001 (2013).

[34] P. Zubko, G. Catalan, and A. K. Tagantsev, Flexoelectric effect in solids, Annu. Rev. Mater. Res. **43**, 387 (2013).

[35] X. T. Zhang, Q. Pan, D. X. Tian, W. F. Zhou, P. Chen, H. F. Zhang, and B. J. Chu, Large Flexoelectriclike Response From the Spontaneously Polarized Surfaces in Ferroelectric Ceramics, Phys. Rev. Lett. **121**, 057602 (2018).

[36] J. F. Scott, Lattice perturbations in $CaWO_4$ and $CaMoO_4$, J. Chem. Phys. **48**, 874 (1968).

[37] S. M. Kogan, Piezoelectric effect during inhomogeneous deformation and acoustic scattering of carriers in crystals, Sov, Phys. Solid State **5**, 2069 (1964).

[38] A. K. Tagantsev, Piezoelectricity and flexoelectricity in crystalline dielectrics, Phys. Rev. B **34**, 5883 (1986).

[39] G. M. Lu, S. Z. Li, X. D. Ding, and E. K. H. Salje, Piezoelectricity and electrostriction in ferroelastic materials with polar twin boundaries and domain junctions, Appl. Phy. Lett. **114**, 202901 (2019).

[40] G. M. Lu, S. Z. Li, X. D. Ding, J. Sun, and E. K. H. Salje, Ferroelectric switching in ferroelastic materials with rough surfaces, Sci. Rep. **9**, 15834 (2019).

[41] M. Stengel, Surface control of flexoelectricity, Phys. Rev. B **90**, 201112 (2014).

[42] A. S. Yurkov and A. K. Tagantsev, Strong surface effect on direct bulk flexoelectric response in solids, Appl. Phy. Lett. **108**, 022904 (2016).

[43] A. Schiaffino, C. E. Dreyer, D. Vanderbilt, and M. Stengel, Metric wave approach to flexoelectricity within density functional perturbation theory, Phys. Rev. B **99**, 085107 (2019).

[44] B. J. Chu, W. Y. Zhu, N. Li, and L. E. Cross, Flexure mode flexoelectric piezoelectric composites, J. Appl. Phy. **106**, 104109 (2009).

[45] J. J. Wortman and R. A. Evans, Young's modulus, shear modulus, and Poisson's ratio in silicon and germanium, J. Appl. Phy. **36**, 153 (1965).

[46] B. J. Chu and D. R. Salem, Flexoelectricity in several thermoplastic and thermosetting polymers, Appl. Phys. Lett. **101**, 103905 (2012).

[47] R. E. Newnham, D. P. Skinner, and L. E. Cross, Connectivity and piezoelectric-pyroelectric composites, Mat. Res. Bull. **13**, 525 (1978).